High-Sensitivity Photodetectors Based on Multilayer GaTe Flakes

Fucai Liu,[†,*] Hidekazu Shimotani,[‡,*] Hui Shang,[‡] Thangavel Kanagasekaran,[†] Viktor Zólyomi,[§] Neil Drummond,[§] Vladimir I. Fal'ko,[§] and Katsumi Tanigaki[†,‡,*]

[†]WPI-Advanced Institute for Materials Research (AIMR), Tohoku University, Sendai 980-8577, Japan, [‡]Department of Physics, Tohoku University, Sendai 980-8577, Japan, and [§]Physics Department, Lancaster University, Lancaster LA1 4YB, United Kingdom

ABSTRACT Optoelectronic devices based on layered materials such as graphene have resulted in significant interest due to their unique properties and potential technological applications. The electric and optoelectronic properties of nano GaTe flakes as layered materials are described in this article. The transistor fabricated from multilayer GaTe shows a p-type action with a hole mobility of about 0.2 $cm^2 V^{-1} s^{-1}$. The gate transistor exhibits a high photoresponsivity of 10^4 A/W, which is greatly better than that of graphene, MoS_2, and other layered compounds. Meanwhile, the response speed of 6 ms is also very fast. Both the high photoresponsivity and the fast response time described in the present study strongly suggest that multilayer GaTe is a promising candidate for future optoelectronic and photosensitive device applications.

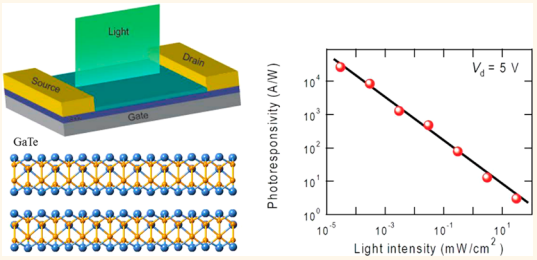

KEYWORDS: gallium telluride · layered material · transistor · photodetector · responsivity

Since the discovery of graphene, layered materials have attracted a lot of interest in various applications, including nanoelectronics, optoelectronics, and energy conversion.[1−3] Graphene has been most intensively studied because of its unique and fascinating physical, chemical, optical, and mechanical properties.[4−7] However, the absence of a band gap restricts its applications, not only for field effect transistors due to the low on/off current ratio, but also for optoelectronics.[8] Especially in the latter applications, graphene absorbs light with about 2% in the range of visible light, and this is too low to use for practical photodetection.[9,10] The absorption intensity can be increased by employing multiply stacking graphene such as bilayer and trilayer graphene sheets, but such an approach by opening a band gap could merely compromise the two important properties of graphene—high transport mobility *via* the Dirac-cone quantum state and the gate bias tunability.[11] Various approaches have recently been proposed, such as exploiting metallic plasmonics, chemical modifications of graphene, and a nanostructured microcavity in order to enhance the light absorption of graphene,[12−14] but the performance of graphene-based photodetectors has not been obviously improved. The fast quenching of photoexcited carriers and the difficult control in the p−n or the metal−graphene junction are the main reasons for the low photoresponsivity of graphene.

As another approach, heterostructures constructed from graphene and other layered materials have been proposed.[15,16] A graphene/WS_2/graphene heterostructure has been demonstrated to exhibit a photoresponsivity of 0.1 A/W.[17] Most recently, a phototransistor based on the graphene−MoS_2 heterostructure reached a photoresponsivity of 10^7 A/W,[18] but this caused a reduction in response speed. In addition, the fabrication processes for making such heterostructures are not generally feasible and will not be compatible with current circuit-fabrication technology in complementary metal-oxide semiconductor electronics. Other layered materials exhibiting exotic properties have been sought to date, such as boron nitride[19,20] and transition-metal dichalcogenide.[21,22] Because of the high electron mobility, the excellent on/off ratio, and the high quantum luminescence efficiency, monolayer MoS_2 has been an interesting research topic nowadays.[23,24]

* Address correspondence to fucai.liu@sspns.phys.tohoku.ac.jp, shimotani@sspns.phys.tohoku.ac.jp, tanigaki@sspns.phys.tohoku.ac.jp.

Received for review October 16, 2013 and accepted December 23, 2013.

Published online December 23, 2013
10.1021/nn4054039

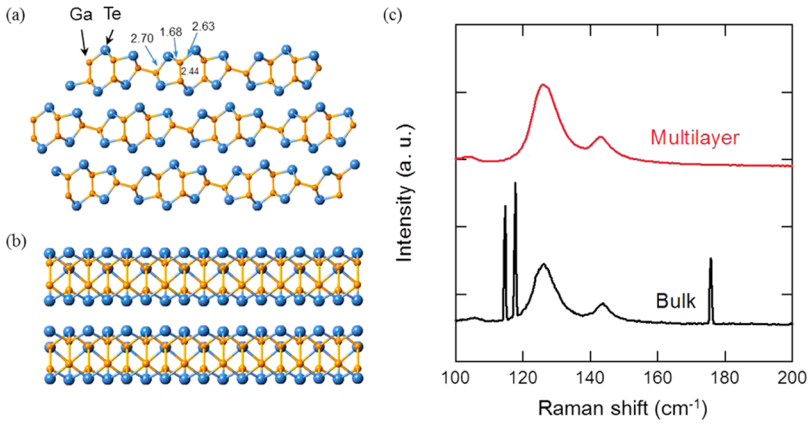

Figure 1. Crystal structure of GaTe: (a) top view and (b) side view; the tellurium and gallium atoms are represented by blue and orange spheres, respectively. Two thirds of the Ga−Ga bonds lie perpendicular to the layer plane; the other one-third lie in the layer plane. The length of the Ga−Ga bond is 2.44 Å; the lengths of Ga−Te bonds are 2.70, 1.68, and 2.63 Å, respectively. (c) Raman spectra of GaTe bulk crystal and multilayer. With decreasing thickness, some peaks are diminished in the multilayer sample.

Via the quantum-mechanical confinement, the band gap of MoS_2 changes from indirect in bulk to direct in monolayer,[25] which makes monolayer MoS_2 suitable for applications in optoelectronic devices. Photodetectors based on monolayer MoS_2 have shown a reasonably high photoresponsivity of up to 880 A/W,[26] but a slow photoresponse time (on the order of several seconds), and the complicated processes of fabricating monolayer MoS_2 devices, however, significantly limit its applications. Moreover, unfortunately the multilayer MoS_2-based photodetectors did not show high photoresponsivity (about 0.1 A/W),[27,28] partly because of its indirect band gap nature.

It can be considered that the direct band gap materials will allow both a high absorption coefficient and efficient electron−hole pair generation under photoexcitation, and therefore a layered material with a natural direct band gap could be a promising candidate for photodetector optoelectronics applications. Keeping this fundamental scenario in mind, gallium telluride GaTe and In_2Se_3 are found to be very intriguing since both are compounds having a direct band gap among III−VI layered semconductors.[29,30] We started experiments along this thought using GaTe nanoflakes by employing the Scotch-tape exfoliation method used in graphene. During the research we made many literature surveys, and a preliminary study was found in a Chinese patent opened to the public very recently.[31] As far as we know from this patent, GaTe was studied as a photodetector with a simple two-terminal contact structure under photoirradiation as one of a series of layered materials, without special attention to the direct band gap.

In the present article, we will report the optoelectronic properties of multilayer GaTe flakes using the field effect transistor device construction and will describe their important physical parameters as a photodetector. It is shown that the GaTe multilayer phototransistor reaches a photoresponsivity value higher than 10^4 A/W, which is 2 orders higher than that of the MoS_2 phototransistor device.[26] In addition, the photoresponse time is about 6 ms, one of the fastest among the reported layered material phototransistors so far. The present results clearly demonstrate that multilayer GaTe thin films are an attractive candidate for applications in optoelectronics.

RESULTS AND DISCUSSION

Layered GaTe has high potential for applications in various optoelectronic devices, radiation detectors, and solar cells due to the optimum band gap as a solar window material and wide band gap as semi-insulating at room temperature. It is a typical III−VI layered semiconductor, with a monoclinic structure and a direct band gap of about 1.7 eV at the Z point of the Brillouin zone border.[32] The unique crystal structure of GaTe induces interesting consequences on the band structure and hence the optical and electrical properties, such as direct band gap and strong excitonic absorption. Figure 1a and b show its crystal structure, and the layer of GaTe consists of alternate Te−Ga−Ga−Te sheets. The chemical bonding between layers is of van der Waals type, while the intralayer atoms are predominantly covalently bonded. The strong covalent bonding in a layer and the weak interlayer van der Waals interactions are responsible for the structural, electric, and optical properties with two-dimensional character in this system. Besides the common in-plane−out-of-plane anisotropy observed in the optical and the electrical properties of layered compounds, the special in-plane anisotropy in the bonding of GaTe makes this material greatly more attractive. In typical III−VI layered compounds such as GaS and GaSe,[33] all Ga−Ga bonds are perpendicular to the layer planes, while GaTe has only two-thirds of the Ga−Ga bonds normal to the layer planes and the others order almost parallel

to them, which results in largely different optical and crystallographic properties from those of the other III–VI compounds. For example, GaS and GaSe are known to be indirect band gap semiconductors,[34,35] in contrast to GaTe, with a direct band gap, and this becomes more advantageous when optoelectronic applications are considered.

Multilayer GaTe flakes can be exfoliated from a bulk crystal by employing the Scotch tape method, which has been extensively adopted in graphene research.[2] The thin flakes were subsequently transferred on a doped silicon substrate covered with a 300 nm thick thermal oxide layer. An optical microscope was used to identify the thin flakes. In the present study, we focused on the multilayer samples (thickness of more than 5 nm) because the yield of the monolayer was found to be much lower than multilayers. We first measured the Raman spectra of GaTe in a multilayer and in bulk, as shown in Figure 1c. The Raman spectra are nearly identical with the data in previous reports,[36–38] indicating that the prepared samples are of reasonably high quality. The peaks at 114.7, 117.8, 126.1, and 143.4 cm^{-1} are the A_g mode, while the peak at 175.8 cm^{-1} is the B_g mode. With decreasing thickness of the sample, only the peaks at 126.1 and 143.4 cm^{-1} remain, while all the other peaks diminished. The observed dependence of the Raman spectrum on layer thickness is still unclear, and more experimental and theoretical approaches will be needed for further clarification.

Theory predicts that when GaTe is thinned to a monolayer, the direct band gap becomes indirect.[39,40] In order to understand the transition from a direct to an indirect gap, we performed first-principles calculations to determine how the band gap in multilayer GaTe approaches that of bulk GaTe. Here it is essential to note that while monolayer GaTe is hexagonal, bulk GaTe is monoclinic (see Figure 1). We have found that the band gap of multilayer hexagonal GaTe rapidly approaches that of bulk hexagonal GaTe, which however is still an indirect band gap. This means that hexagonal GaTe always has an indirect band gap regardless of the number of layers; therefore we conclude that the samples in our experiment exist in the monoclinic phase, just like bulk GaTe. It is worth noting however that in the hexagonal phase an important shift takes place in the valence band. The valence band maximum shifts toward the Γ point as the number of layers is increased (see Figure 2), and by the time we reach a width of 10 layers (which is the thickness of our thinnest sample) it shifts all the way to the Γ point, allowing for an optical transition with the local conduction band minimum at Γ. Therefore, even in a hexagonal phase it is reasonable to expect improved optical absorption efficiency and a good optoelectronic performance in multilayer GaTe. A more detailed calculation including the geometrical optimization

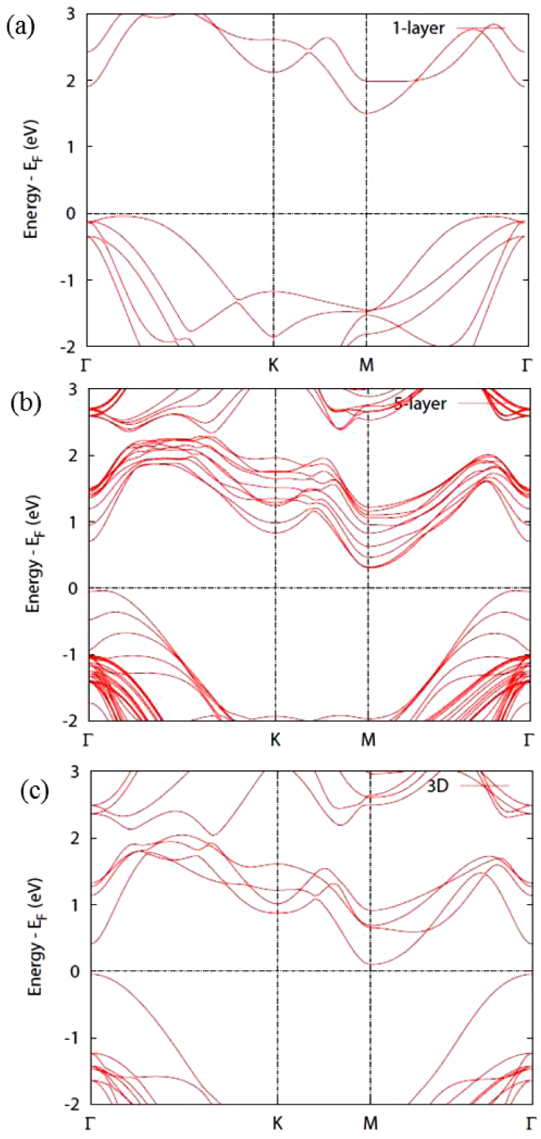

Figure 2. Band structures of GaTe with a thickness of (a) monolayer, (b) five layers, and (c) bulk, based on the hexagonal crystal structure.

without any structural constraints and a comparison between experiment and theory would be very intriguing in future studies. As a cross check we have also calculated the band structure of single-layer monoclinic GaTe using fixed lattice paramaters taken from the bulk 3D monoclinic material, and we found that it exhibits a direct band gap just like the bulk 3D monoclinic phase, which indicates that multilayer monoclinic GaTe should have a direct band gap, in accordance with our measurements.

Regarding the Raman spectra, the persistence of the two peaks at 126.1 and 143.4 cm^{-1} suggests that they are Γ point phonons originating from a single layer perturbed only slightly by the van der Waals interaction. As such, it makes sense to compare the results to first-principles calculations,[40] which show that hexagonal GaTe has five zone center Raman active modes

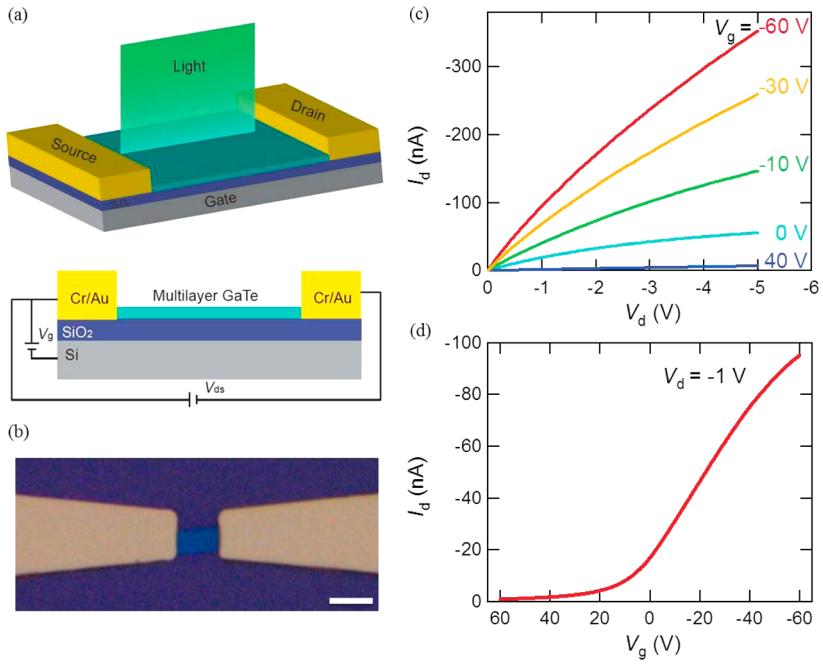

Figure 3. (a) Three-dimensional schematic view and the cross section view of the multilayer GaTe device. A doped silicon substrate covered with 300 nm thick SiO_2 was used as a back gate. The Cr/Au electrodes were used as source and drain. (b) Optical image of a typical multilayer GaTe device. Scale bar is 10 μm. The thickness of the flake is about 10 nm. (c) Output and (d) transfer curves of a multilayer GaTe transistor. The transistor shows p-type behavior, and the mobility deduced from the transfer curves is about 0.2 $cm^2 V^{-1} s^{-1}$.

with three of them at frequencies above 180 cm^{-1}. This does not agree with the measurements and is therefore further evidence that the samples in our measurements are in the monoclinic and not in the higher symmetry hexagonal phase.

Before discussing the photoresponse behavior, we examine the electrical transport properties of a GaTe transistor at room temperature. Figure 3a and b show a schematic view and an optical image of the multilayer device fabricated by photolithography, where two Cr/Au electrodes were deposited as the source and the drain, respectively. Figure 3c and d show the output and the transfer characteristics of the fabricated transistor. It can be seen from the figure that the transistor exhibited an obvious p-type semiconducting behavior, which is consistent with previous reports. The field effect mobility of this device was estimated from the linear region in the I_d-V_g curve by using the equation $\mu = (dI_d)/(dV_g) \times L/(WC_iV_d)$, where L is the channel length, W is the channel width, and C_i is the capacitance between the channel and the back gate per unit area ($C_i = \varepsilon_0\varepsilon_r/d$; ε_0 is the vacuum permittivity, ε_r is the relative permittivity, and d is the thickness of SiO_2 layer). The calculated mobility of our device was about 0.2 $cm^2 V^{-1} s^{-1}$, and this is comparable with that of other compounds such as GaS, GaSe, and MoS_2.[41] It is well known that trap/impurity states exist on the SiO_2/Si surface in the case of bottom gate transistors and that scattering from the charged impurities degrades the carrier mobility of the devices. Reducing the amount of surface traps/impurities in the bottom gate dielectric is expected to improve the mobility of the GaTe-based transistors. It has been reported that the mobility of MoS_2 can be increased from 0.1 to 200 $cm^2 V^{-1} s^{-1}$ by using the high-k gate dielectric material HfO_2 as a top gate due to the suppression of Coulomb scattering as well as the modification of phonon dispersion.[23] In addition, the channel layer thickness and the contact resistance also play key roles in obtaining high-mobility and high-performance transistors.[42,43] Further improvement of the mobility will be achieved by optimizing these conditions in GaTe transistors.

The optoelectronic properties of multilayer GaTe-based phototransistors were investigated by exploring their output characteristics of the photocurrent, such as the photocurrent generation and the photoresponsivity at different light intensities, and different applied drain and gate voltages. To generate the photocurrent, the incident photon energy must be greater than the energy gap of the intrinsic semiconductor, and the response of photodetectors is proportional to the rate of incident beams of photons. Since the energy of a photon is inversely proportional to the wavelength, the spectral response generally increases linearly with the wavelength. Light in the green wavelength region is of special interest and has a very wide range of applications. For example, X-ray images in radiology operate at the green wavelength region. Therefore, a fast photodetector with good performance at the green wavelength would significantly advance the state of the art and expand the usage of imaging applications.

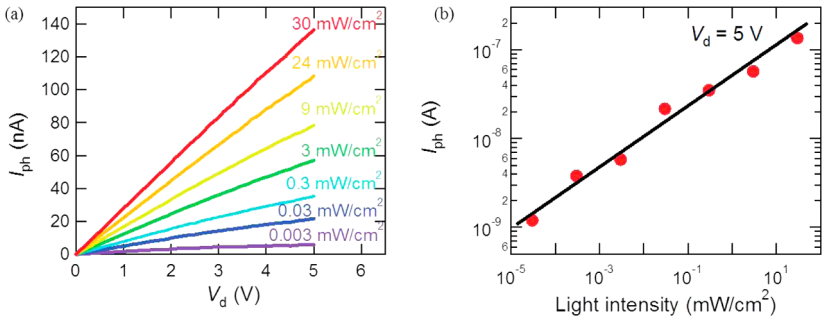

Figure 4. (a) Photocurrent as a function of the drain voltage under the illumination of different light intensities at a wavelength of 532 nm. (b) Light intensity dependence of the photocurrent under a drain voltage of 5 V. The photocurrent has a power law dependence on the light intensity. The black line is the guide to the eyes.

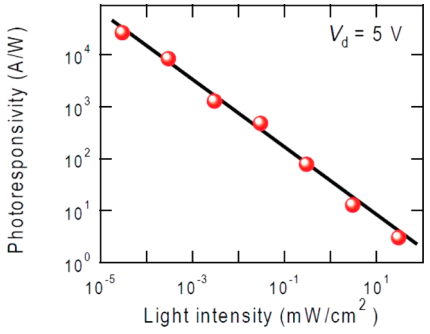

Figure 5. Dependence of the photoresponsivity on the illuminated light intensity. The photoresponsivity is deduced from the data of Figure 4b. The black line is the guide to the eyes. The light wavelength is 532 nm and the drain voltage is 5 V. At a low light intensity, the photoresponsivity exceeds 10^4 A/W.

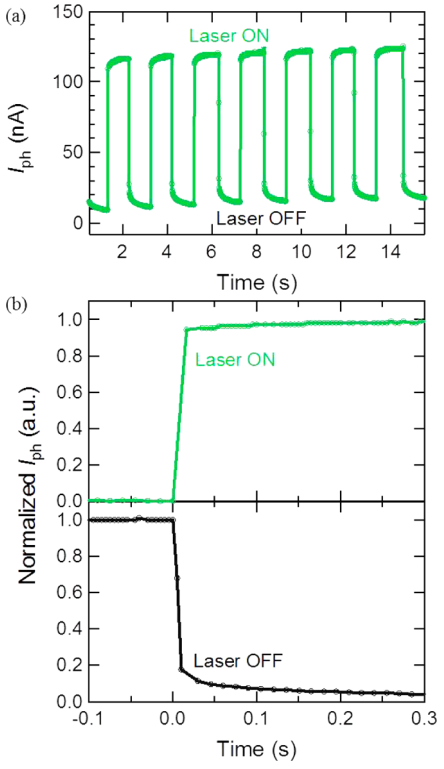

Figure 6. (a) Time-resolved photoresponse of the multilayer GaTe device recorded by alternative switching on and off the light illumination. (b) Typical rise or decay behaviors of the photocurrent at the initial stage just after the light illumination is switched on (upper panel) or off (lower panel). The photocurrent and the time are normalized and shifted. The photocurrent increases (decreases) more than 90% in 20 ms after the light illumination is switched on (off).

In the present study, we chose 532 nm as the illumination source wavelength for studying the GaTe-based photodetector.

We first studied the light intensity dependence of the photocurrent. Figure 4a shows that the photocurrent changes as a function of drain voltage at various light intensities under exposure to the 532 nm light. Under this excitation energy, the device still generates an obvious photocurrent even if the illumination intensity is less than 30 nW/cm^2. Remarkably, the device shows a response in a wide range of light intensity from tens of nW/cm^2 to 30 mW/cm^2. This is thanks to the high transition probability due to the direct band gap of GaTe. The photocurrent increases gradually as the light intensity increases. In Figure 4b, we plot the light intensity dependence of the photocurrent in a log−log scale. It can clearly be seen that the photocurrent can be expressed by a simple power law equation, $I_{ph} \propto p^{\alpha}$, where I_{ph} is the photocurrent, P is the light intensity, and α is the index of a power law. By fitting the experimental data in Figure 4b, the α value was deduced to be 0.73. The deviation from the ideal slope of $\alpha = 1$ is attributed to complex processes in the carrier generation, trapping, and electron−hole recombination in the semiconductor.[44]

One of the most important parameters for a photodetector is its photoresponsivity R, which is the ratio of generated photocurrent intensity to that of the incident light.[45] Figure 5 shows the photoresponsivity R evaluated at a bias voltage of 5 V. At low illumination intensities, the present device reached a photoresponsivity of 10^4 A/W, and this value is several orders higher than that of graphene-based photodetectors as well as that of MoS_2-based photodetectors reported elsewhere.[26] A sublinear dependence of the photoresponse on the light intensity was observed upon tuning the light intensity. The presence of the trap states either in GaTe or at the interface between GaTe and the underlying

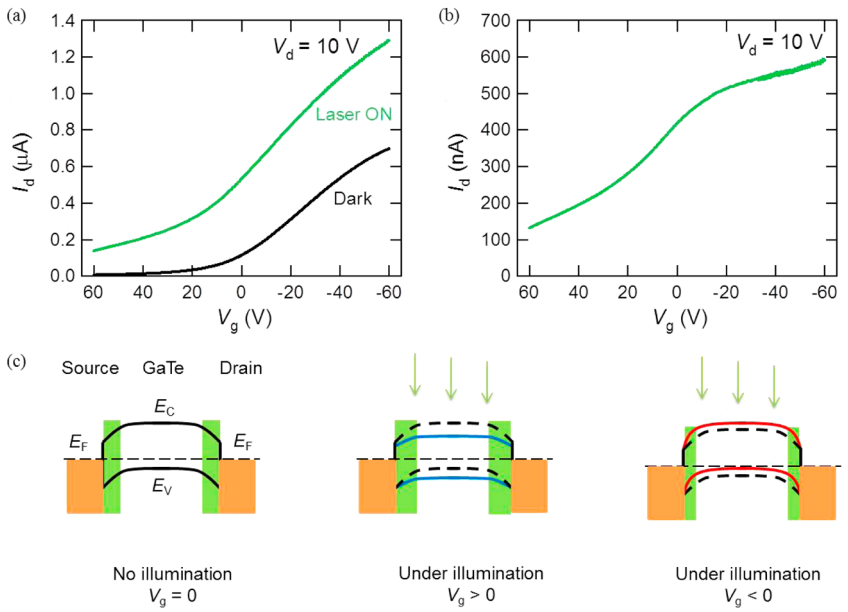

Figure 7. (a) Gate voltage dependences of the drain current under dark state (black line) and under light illumination (green line). The light wavelength is 532 nm, and the light intensity is about 30 mW/cm^2. Applied drain voltage is 10 V. (b) Dependence of photocurrent on the gate voltage deduced from (a). (c) Schematic band diagram of the devices under different illumination and gate bias conditions. E_F, Femi level; E_C, conduction band; E_V, valence band. Green area indicates the thickness of the Schottky barrier. Depending on the applied gate voltage, the thickness of the Schottky barrier can be increased or reduced, resulting in the gate dependence of the photocurrent.

SiO_2 layer may be responsible for such a reduction in photoresponsivity. The reduction in the density of electron trapping states under high illumination intensity led to the saturation of the photoresponse.[26] On the other hand, the carrier lifetime will be shortened due to the self-collisions and quenching of photogenerated carriers under high light-power illumination.[46]

The response time is the critical factor for realizing a high-performance photodetector. In the present study we investigated a time-resolved photocurrent change by the light illumination cycles with on and off modes. The photocurrent changing as a function of time under this process is shown in Figure 6a. The photocurrent was modulated depending on the light illumination period on or off. In order to understand the fast response of the photocurrent, the photocurrent in the initial stage of light illumination with both on and off modes was recorded and shown in Figure 6b. In the first 20 ms after the illumination was turned on or off, the photocurrent changed (rose or decayed) by more than 90%. The photocurrent rose dramatically in 20 ms after the light illumination and then increased with a little slower kinetics. The photocurrent also decayed very fast within 20 ms after the light-off, followed by slow kinetics before returning back to the initial dark current. The response dynamics of the photocurrent in our devices can be described by an exponential function, and the response time constant can be deduced by fitting the experimental data. The evaluated rise time constant was about 6 ms, which is one of the fastest among the data so far reported for layered material-based photodetectors.[47] This value is still larger than that usually observed for the intrinsic band-to-band excitations in conventional bulk semiconductors. This can be attributed to the influences of traps and other defect states during the photocurrent generation processes.

Finally the gate bias tunability of the photoresponse will be described. The photocurrent generation was recorded by monitoring the drain current (I_d) under illumination by scanning the gate voltage (V_g) from 60 to −60 V, keeping both the light intensity and the drain voltage constant. The gate voltage dependence of the photocurrent was observed and shown in Figure 7b. The photocurrent gradually increases when changing the gate voltage from positive to negative. The gate voltage dependence of the photocurrent is consistent with that of the p-type-doped GaTe. Because the Cr adhesion layer (3 nm) is extremely thin and does form a continuous film, as schematically illustrated in Figure 7c, we restrict our discussion to the Au and GaTe interface. When Au electrode and GaTe are contacted, a charge transfer occurs at the interfaces *via* Femi level tuning under an equilibrium condition, and this causes the accumulation of space charge in the contact region together with band bending to form a Schottky-type barrier as well as a depletion layer. When a positive gate voltage is applied, the band shifts downward and the depletion layer increases simultaneously, resulting in the larger Schottky barrier. The tunneling of photocarriers through the Schottky

TABLE 1. Summary of Important Device Parameters of Photodetectors Based on Layered Materials Including This Work

material	device structure	spectral range	responsivity	response time	ref
graphene	3 terminal	visible IR	0.01 A/W	1.5 ps	5
graphene oxide	3 terminal	IR	0.7 A/W	2 s	48
monolayer MoS_2	3 terminal	visible	880 A/W	4 s	26
multilayer MoS_2	3 terminal	UV−IR	0.1 A/W		27
multilayer WS_2	2 terminal	visible	92 μA/W	5 ms	47
multilayer GeSe	3 terminal	visible		few seconds	49
multilayer GaSe	2 terminal	UV−visible	2.8 A/W	20 ms	50
multilayer GaTe	3 terminal	visible	10^4 A/W	6 ms	this work
ZnO needle	3 terminal	UV	4700 A/W		51
Si	2 terminal	UV−visible	119 A/W		52

barrier becomes more difficult than the zero gate voltage condition. On the other hand, the Schottky barrier will become narrow when negative gate voltage is applied, and the photogenerated charges will drift efficiently to the external circuit accompanied by a large photocurrent.

In order to compare the photoresponse properties of GaTe with those of other layered materials, we summarized the photoresponsivity and the response time in Table 1, both of which are two crucial factors for photodetection devices, together with the data of other layered compounds reported in the literature. A comparison with other semiconductors such as ZnO and Si is also made. As can be seen from Table 1, graphene and multilayer WS_2 have the shortest response time, but their photoresponsivities are very low. Monolayer MoS_2 exhibits a very high photoresponsivity, but instead the response speed decreases. In contrast, multilayer GaTe shows a high photoresponsivity and a fast response speed and, therefore, is very promising for photodetector applications.

CONCLUSIONS

In conclusion, we studied the electronic and photoresponsive properties of GaTe multilayer nanoflakes. A GaTe transistor showed a p-type operation with a hole mobility of about 0.2 $cm^2 V^{-1} s^{-1}$. Because of the direct band gap of GaTe, the photosensitive device based on GaTe exhibited a very high photoresponsivity of 10^4 A/W, which is 2 orders of magnitude higher than that of the MoS_2 photodetector. In addition the device showed very fast photoresponse dynamics with a response time of less than 20 ms, and it was tuned by the back gate voltage. Owing to both large-scale material preparation methods, such as liquid exfoliation[53] and CVD method,[54] and simple device fabrication processes, multilayer GaTe nanoflakes will be a promising material for applications in optoelectronics and could provide low-cost and flexible optoelectronic devices.

METHODS

Multilayer GaTe nanoflakes were mechanically exfoliated from bulk GaTe crystals (2D semiconductors) by the Scotch tape method, transferred on SiO_2/Si substrates, and then characterized by Raman spectroscopy (Horiba, LabRAM HR-800), optical microscopy (Olympus, BX51), and atomic force microscopy (Hitachi, AFM5100N). The devices were fabricated by conventional photolithography, evaporation, and lift off processes. Cr (3 nm) and Au (60 nm) were deposited by thermal deposition under high vacuum. Electric performances were measured by current−voltage measurements using a semiconductor parameter analyzer (Agilent, B1500A). A semiconductor laser with a wavelength of 532 nm was used to study the photoresponse properties of the devices. First-principles calculations were performed using the VASP[55] plane-wave-based density functional theory code within the local density approximation with a 600 eV plane-wave cutoff energy and a 12 × 12 Monkhorst-Pack k-point grid (12 × 12 × 12 in the case of bulk hexagonal GaTe).

Conflict of Interest: The authors declare no competing financial interest.

Acknowledgment. This research was financially supported by MEXT of Japan (No. 24651128 and No. 24684023). F.L. acknowledges the financial support of the AIMR fusion research project. V.Z. acknowledges the Marie Curie grant CARBOTRON.

REFERENCES AND NOTES

1. Novoselov, K. S.; Geim, A. K.; Morozov, S. V.; Jiang, D.; Zhang, Y.; Dubonos, S. V.; Firsov, A. A. Electric Field Effect in Atomically Thin Carbon Films. *Science* **2004**, *306*, 666–669.
2. Novoselov, K. S.; Jiang, D.; Schedin, F.; Booth, T. J.; Khotkevich, V. V.; Morozov, S. V.; Geim, A. K. Two-Dimensional Atomic Crystals. *Proc. Natl. Acad. Sci. U.S.A.* **2005**, *102*, 10451–10453.
3. Wang, Q. H.; Kalantar-Zadeh, K.; Kis, A.; Coleman, J. N.; Strano, M. S. Electronics and Optoelectronics of Two-Dimensional Transition Metal Dichalcogenides. *Nat. Nanotechnol.* **2012**, *7*, 699–712.
4. Bonaccorso, F.; Sun, Z.; Hasan, T.; Ferrari, A. C. Graphene Photonics and Optoelectronics. *Nat. Photonics* **2010**, *4*, 611–622.
5. Sun, D.; Aivazian, G.; Jones, A. M.; Ross, J. S.; Yao, W.; Cobden, D.; Xu, X. Ultrafast Hot-Carrier-Dominated Photocurrent in Graphene. *Nat. Nanotechnol.* **2012**, *7*, 114–118.
6. Pospischil, A.; Humer, M.; Furchi, M. M.; Bachmann, D.; Guider, R.; Fromherz, T.; Mueller, T. CMOS-Compatible Graphene Photodetector Covering All Optical Communication Bands *Nat. Photonics* **2013**, DOI: 10.1038/nphoton.2013.240.
7. Novoselov, K. S; Jiang, Z.; Zhang, Y.; Morozov, S. V.; Stormer, H. L.; Zeitler, U.; Maan, J. C.; Boebinger, G. S.; Kim, P.; Geim, A. K. Room-Temperature Quantum Hall Effect in Graphene. *Science* **2007**, *315*, 1379.
8. Schwierz, F. Graphene Transistors. *Nat. Nanotechnol.* **2010**, *5*, 487–496.
9. Mueller, T.; Xia, F. N.; Avouris, P. Graphene Photodetectors for High-Speed Optical Communications. *Nat. Photonics* **2010**, *4*, 297–301.
10. Nair, R. R.; Blake, P.; Grigorenko, A. N.; Novoselov, K. S.; Booth, T. J.; Stauber, T.; Peres, N. M. R.; Geim, A. K. Fine Structure Constant Defines Visual Transparency of Graphene. *Science* **2008**, *320*, 1308.
11. Zhou, S. Y.; Gweon, G. H.; Fedorov, A. V.; First, P. N.; De Heer, W. A.; Lee, D. H.; Guinea, F.; Castro Neto, A. H.; Lanzara, A. Substrate-Induced Bandgap Opening in Epitaxial Graphene. *Nat. Mater.* **2007**, *6*, 770–775.

12. Koppens, F. H. L.; Chang, D. E.; García de Abajo, F. J. Graphene Plasmonics: A Platform for Strong Light−Matter Interactions. *Nano Lett.* **2011**, *11*, 3370–3377.
13. Furchi, M.; Urich, A.; Posposchil, A.; Lilley, G.; Unterrainer, K.; Detz, H.; Klang, P.; Andrews, A. M.; Schrenk, W.; Strasser, G.; *et al*. Microcavity-Integrated Graphene Photodetector. *Nano Lett.* **2012**, *12*, 2773–2777.
14. Engel, M.; Steiner, M.; Lombardo, A.; Ferrari, A. C.; von Löhneysen, H.; Avouris, P.; Krupke, R. Light−Matter Interaction in a Microcavity-Controlled Graphene Transistor. *Nat. Commun.* **2012**, *3*, 906.
15. Ponomarenko, L. A.; Geim, A. K.; Zhukov, A. A.; Jalil, R.; Morozov, S. V.; Novoselov, K. S.; Grigorieva, I. V.; Hill, E. H.; Cheianov, V. V.; Falko, V. I.; *et al*. Tunable Metal-Insulator Transition in Double-Layer Graphene Heterostructures. *Nat. Phys.* **2011**, *7*, 958–961.
16. Georgiou, T.; Jalil, R.; Belle, B. D.; Britnell, L.; Gorbachev, R. V.; Morozov, S. V.; Kim, Y.-J.; Gholinia, A.; Haigh, S. J.; Makarovsky, O.; *et al*. Vertical Field Effect Transistor Based on Graphene-WS2 Heterostructures for Flexible and Transparent Electronics. *Nat. Nanotechnol.* **2013**, *8*, 100–103.
17. Britnell, L.; Ribeiro, R. M.; Eckmann, A.; Jalil, R.; Belle, B. D.; Mishchenko, A.; Kim, Y.-J.; Gorbachev, R. V.; Georgiou, T.; Morozov, S. V. Strong Light-Matter Interactions in Heterostructures of Atomically Thin Films. *Science* **2013**, *340*, 1311–1314.
18. Zhang, W.; Chuu, C.; Huang, J.; Chen, C.; Tsai, M.; Chang, Y.; Liang, C.; He, J.; Chou, M.; Li, L. Ultrahigh-Gain Phototransistors Based on Atomically Thin Graphene-MoS_2 Heterostructures. *Adv. Mater.* **2013**, adma.201302859.
19. Alem, N.; Erni, R.; Kiselowski, C.; Rossell, M. D.; Gannett, W.; Zettl, A. Atomically Thin Hexagonal Boron Nitride Probed by Ultrahigh-Resolution Transmission Electron Microscopy. *Phys. Rev. B* **2009**, *80*, 155425.
20. Lee, C.; Li, Q.; Kalb, W.; Liu, X.-Z.; Berger, H.; Carpick, R. W.; Hone, J. Frictional Characteristics of Atomically Thin Sheets. *Science* **2010**, *328*, 76–80.
21. Chhowalla, M.; Shin, H. S.; Eda, G.; Li, L.-J.; Loh, K. P.; Zhang, H. The Chemistry of Two-Dimensional Layered Transition Metal Dichalcogenide Nanosheets. *Nat. Chem.* **2013**, *5*, 263–275.
22. Jones, A. M.; Yu, H.; Ghimire, N.; Wu, S.; Aivazian, G.; Ross, J. S.; Xu, X. Optical Generation of Excitonic Valley Coherence in Monolayer WSe_2. *Nat. Nanotechnol.* **2013**, *8*, 634–638.
23. Radisavljevic, B.; Radenovic, A.; Brivio, J.; Giacometti, V.; Kis, A. Single-Layer MoS_2 Transistors. *Nat. Nanotechnol.* **2011**, *6*, 147–150.
24. Kim, S.; Konar, A.; Hwang, W.-S.; Lee, J. H.; Lee, J.; Yang, J.; Jung, C.; Kim, H.; Yoo, J.-B.; Choi, J.-Y.; *et al*. High-Mobility and Low-Power Thin-Film Transistors Based on Multilayer MoS_2 Crystals. *Nat. Commun.* **2012**, *3*, 1011.
25. Mak, K. F.; Lee, C.; Hone, J.; Shan, J.; Heinz, T. F. Atomically Thin MoS_2: A New Direct-Gap Semiconductor. *Phys. Rev. Lett.* **2010**, *105*, 136805.
26. Lopez-Sanchez, O.; Lembke, D.; Kayci, M.; Radenovic, A.; Kis, A. Ultrasensitive Photodetectors Based on Monolayer MoS_2. *Nat. Nanotechnol.* **2013**, *8*, 497–501.
27. Choi, W.; Cho, M. Y.; Konar, A.; Lee, J. H.; Cha, G. B.; Hong, S. C.; Kim, S.; Kim, J. Y.; Jena, D.; Joo, J.; *et al*. High-Detectivity Multilayer MoS_2 Phototransistors with Spectral Response from Ultraviolet to Infrared. *Adv. Mater.* **2012**, *24*, 5832–5836.
28. Lee, H. S.; Min, S.-W.; Chang, Y.-G.; Park, M. K.; Nam, T.; Kim, H.; Kim, J. H.; Ryu, S.; Im, S. MoS_2 Nanosheet Phototransistors with Thickness-Modulated Optical Energy Gap. *Nano Lett.* **2012**, *12*, 3695–3700.
29. Camassel, J.; Merle, P.; Mathieu, H. Exciton Absorption Edge of GaTe. *Physica B+C* **1980**, *99*, 309–313.
30. Julien, C.; Cheavy, A.; Siapkas, D. Optical Properties of In_2Se_3 Phases. *Phys. Status Solidi A* **1990**, *118*, 553–559.
31. Hu, P. A.; Li. X.; Li, J.; Li. X.; Feng, W.; Wang, X.; Wang, L.; Zhang, J. Gallium Telluride Material Preparation Method and the Two-Dimensional Structure of Gallium Telluride Flexible Transparent Method for Preparing a Photodetector CN Pat. Appl. CN 201310139850, Aug 7, 2013
32. Sánchez-Royo, J. F.; Pellicer-Porres, J.; Segura, A.; Munoz-Sanjoseet, V.; Tobias, G.; Ordejon, P.; Canadell, E.; Huttel, Y. Angle-Resolved Photoemission Study and First-Principles Calculation of the Electronic Structure of GaTe. *Phys. Rev. B* **2002**, *65*, 115201.
33. Plucinski, L.; Johnson, R.; Kowalski, B.; Kopalko, K.; Orlowski, B.; Kovalyuk, Z.; Lashkarev, G. Electronic Band Structure of GaSe(0001): Angle-Resolved Photoemission and *ab Initio* Theory. *Phys. Rev. B* **2003**, *68*, 125304.
34. Ho, C. H.; Lin, S. L. Optical Properties of the Interband Transitions of Layered Gallium Sulfide. *J. Appl. Phys.* **2006**, *100*, 083508.
35. Alekperov, O. Z.; Godjaev, M. O.; Zarbaliev, M. Z.; Suleimanov, R. A. Interband Photoconductivity in Layer Semiconductors GaSe, InSe and GaS. *Solid State Commun.* **1991**, *77*, 65–67.
36. Loudon, R. The Raman Effect in Crystals. *Adv. Phys.* **2011**, *50*, 813–864.
37. Abdullaev, G. B.; Vodopyanov, L. K.; Allakhverdiev, K. R.; Golubev, L. V.; Babaev, S. S.; Salaev, E. Y. Raman Spectra of α-GaTe Single Crystals. *Solid State Commun.* **1979**, *31*, 851–855.
38. Cerdeira, F.; Meneses, E. A.; Gouskov, A. Splittings and Correlations between the Long-Wavelength Optical Phonons in the Layer Compounds GaSe, GaTe, and $GaSe_{1-x}Te_x$. *Phys. Rev. B* **1977**, *16*, 1648–1654.
39. Zhang, H. L.; Hennig, R. G. Single-Layer Group-III Monochalcogenide Photocatalysts for Water Splitting. *Chem. Mater.* **2013**, *25*, 3232–3238.
40. Zolyomi, V.; Drummond, N. D.; Fal'ko, V. I. Band Structure and Optical Transitions in Atomic Layers of Hexagonal Gallium Chalcogenides. *Phys. Rev. B* **2013**, *87*, 195403.
41. Late, D. J.; Liu, B.; Luo, J.; Yan, A.; Matte, H. S. S. R.; Grayson, M.; Rao, C. N. R.; Dravid, V. P. GaS and GaSe Ultrathin Layer Transistors. *Adv. Mater.* **2012**, *24*, 3549–3554.
42. Liu, W.; Kang, J.; Sarkar, D.; Khatami, Y.; Jena, D.; Banerjee, K. Role of Metal Contacts in Designing High-Performance Monolayer n-Type WSe_2 Field Effect Transistors. *Nano Lett.* **2013**, *13*, 1983–1990.
43. Das, S.; Chen, H.-Y.; Penumatcha, A. V.; Appenzeller, J. High Performance Multi-Layer MoS_2Transistors with Scandium Contacts. *Nano Lett.* **2013**, *13*, 100–105.
44. Kind, H.; Yan, H.; Messer, B.; Law, M.; Yang, P. Nanowire Ultraviolet Photodetectors and Optical Switches. *Adv. Mater.* **2002**, *14*, 158–160.
45. Konstantatos, G.; Sargent, E. H. Nanostructured Materials for Photon Detection. *Nat. Nanotechnol.* **2010**, *5*, 391–400.
46. Soci, C.; Moses, D.; Xu, Q. H.; Heeger, A. J. Charge-Carrier Relaxation Dynamics in Highly Ordered Poly(*p*-phenylene vinylene): Effects of Carrier Bimolecular Recombination and Trapping. *Phys. Rev. B* **2005**, *72*, 245204.
47. Perea-López, N.; Elías, A. L.; Berkdemir, A.; Castro-Beltran, A.; Gutiérrez, H. R.; Feng, S.; Terrones, M. Photosensor Device Based on Few-Layered WS_2 Films. *Adv. Funct. Mater.* DOI: 10.1002/adfm.201300760.
48. Chang, H.; Sun, Z.; Saito, M.; Yuan, Q.; Zhang, H.; Li, J.; Wang, Z.; Fujita, K.; Ding, F.; Zheng, Z.; *et al*. Regulating Infrared Photoresponses in Reduced Graphene Oxide Phototransistors by Defect and Atomic Structure Control. *ACS Nano* **2013**, *7*, 6310–6320.
49. Xue, D. J.; Tan, J.; Hu, J. S.; Hu, W.; Guo, Y. G.; Wan, L. J. Anisotropic Photoresponse Properties of Single Micrometer-Sized GeSe Nanosheet. *Adv. Mater.* **2012**, *24*, 4528–4533.
50. Hu, P. A.; Wen, Z.; Wang, L.; Tan, P.; Xiao, K. Synthesis of Few-Layer GaSe Nanosheets for High Performance Photodetectors. *ACS Nano* **2012**, *6*, 5988–5994.
51. Weng, W. Y.; Chang, S. J.; Hsu, C. L.; Hsueh, T. J. A ZnO-Nanowire Phototransistor Prepared on Glass Substrates. *ACS Appl. Mater. Interfaces* **2011**, *3*, 162–166.
52. Huang, Z.; Carey, J. E.; Liu, M.; Guo, X.; Mazur, E.; Campbell, J. C. Microstructured Sillicon Photodetector. *Appl. Phys. Lett.* **2006**, *89*, 033506.
53. Coleman, J. N.; Lotya, M.; O'Neill, A.; Bergin, S. D.; King, P. J.; Khan, U.; Young, K.; Gaucher, A.; De, S.; Smith, R. J.; *et al*.

Two-Dimensional Nanosheets Produced by Liquid Exfoliation of Layered Materials. *Science* **2011**, *331*, 568–571.
54. Lei, S.; Ge, L.; Liu, Z.; Najmaei, S.; Shi, G.; You, G.; Lou, J.; Vajtai, R.; Ajayan, P. M. Synthesis and Photoresponse of Large GaSe Atomic Layers. *Nano Lett.* **2013**, *13*, 2777–2781.
55. Kresse, G.; Furthmüller, J. Efficient Iterative Schemes for *ab Initio* Total-Energy Calculations Using a Plane-Wave Basis Set. *Phys. Rev. B* **1996**, *54*, 11169–11186.